Sala-Mira, I.; García Gil, PJ.; Diez, J.; Bondia, J. (2022). Internal model control based module for the elimination of meal and exercise announcements in hybrid artificial pancreas systems. Computer Methods and Programs in Biomedicine. 226:1-13. https://doi.org/10.1016/j.cmpb.2022.107061

# Internal model control based module for the elimination of meal and exercise announcements in hybrid artificial pancreas systems

Iván Sala-Mira[a], Pedro Garcia[a], José-Luis Díez[a,b], Jorge Bondia[a,b,*]

[a]*Instituto Universitario de Automática e Informática Industrial, Universitat Politècnica de València, 46022, Valencia, Spain*
[b]*Centro de Investigación Biomédica en Red de Diabetes y Enfermedades Metabólicas Asociadas - CIBERDEM, 28028, Madrid, Spain*

## Abstract

*Background and Objectives.* Hybrid artificial pancreas systems outperform current insulin pump therapies in blood glucose regulation in type 1 diabetes. However, subjects still have to inform the system about meals intake and exercise to achieve reasonable control. These patient announcements may result in overburden and compromise controller performance if not provided timely and accurately. Here, a hybrid artificial pancreas is extended with an add-on module that releases subjects from meals and exercise announcements.

*Methods.* The add-on module consists of an internal-model controller that generates a "virtual" control action to compensate for disturbances. This "virtual" action is converted into insulin delivery, rescue carbohydrates sugges-

*Abbreviations:* AP, artificial pancreas; CGM, continuous glucose monitor; CI, confidence interval; IFB, insulin feedback; IMC, internal model control; SMRC, sliding mode reference conditioning;

*Corresponding author

tions, or insulin-on-board limitations, depending on a switching logic based on glucose measurements and predictions. The controller parameters are tuned by optimization and then related to standard parameters from the open-loop therapy. This module is implemented in a hybrid artificial pancreas system proposed by our research group for validation. This hybrid system extended with the add-on module is compared with the hybrid controller with carbohydrate counting errors (hybrid) and the hybrid controller with an alternative unannounced meal compensation module based on a meal detection algorithm (meal detector). The validation used the educational version of the UVa/Padova simulator to simulate the three controllers under two scenarios: one with only meals and another with meals and exercise. The exercise was modeled as a temporal increase of the insulin sensitivity resulting in the glucose drop usually related to an aerobic exercise.

*Results.* For the scenario with only meals, the three controllers achieved similar time in range (proposed: 85.1 [77.9,88.1]%, hybrid: 84.0 [75.9,86.4]%, meal detector: 81.9 [79.3,83.8]%, median [interquartile range]) with low time in moderate hypoglycemia. Under the scenario with meals and exercise, the proposed module reduces 4.61% the time in hypoglycemia achieved with the other controllers, suggesting an acceptable amount of rescues (27.2 [23.7, 31.0] g).

*Conclusions.* The proposed add-on module achieved promising results: it outperformed the meal-detector-based controller, even achieving a postprandial performance as good as the hybrid controller (with carbohydrate counting errors). Also, the rescue suggestion feature of the module mitigated exercise-induced hypoglycemia with admissible rescue amounts.

*Keywords:* type 1 diabetes, artificial pancreas, postprandial control, hypoglycemia avoidance, internal model control, disturbance rejection

## 1. Introduction

Closed-loop glucose control (also known as artificial pancreas) outperforms other insulin therapies treating type 1 diabetes, such as multiple daily insulin therapy or sensor-augmented pump [1, 2]. This technology reduces time in high glucose values (hyperglycemia) and associated risks such as retinopathy, neuropathy, or cardiovascular disease [3, 1]. The artificial pancreas also reduces time in low blood glucose values (hypoglycemia), with critical short-term complications (e.g., cognitive dysfunction, seizures, or coma in severe cases [4]), and enhances the quality of life with reduced anxiety or insomnia [2].

However, external disturbances, namely, meals and exercise, challenge the performance of artificial pancreas systems. On the one hand, glucose ingested from meals reaches the bloodstream faster than subcutaneous insulin. Slow subcutaneous insulin absorption and sensor lag delay the insulin action, leading to sizeable postprandial glucose excursions [5]. Insulin stacked in subcutaneous depots continues to be absorbed even after the meal absorption, which may also cause hypoglycemia [6]. On the other hand, exercise is beneficial for managing type 1 diabetes: it improves insulin sensitivity, reduces cardiovascular risks, improves bones health, etc. [7, 8].However, exercise influences the balance between glucose utilization and production; thus, it may cause hypoglycemia or hyperglycemia, depending on the kind of exercise, its duration, and its intensity [7, 9]. Low-to-moderate aerobic exercise usually

lowers glucose; the fear of subsequent hypoglycemia constitutes the main reason people with type 1 diabetes give up an active lifestyle [9].

Commercially available artificial pancreas systems – a recent review reported up to six systems [10]: the Medtronic 670G (Medtronic, Northridge, CA, USA), the Medtronic 780G (Medtronic, Northridge, CA, USA), the t:slim X2 pump with Control-IQ (Tandem, San Diego, CA, USA), the CamAPS FX (CamDiab, Cambridge, UK), the DBLG1 (Diabeloop, Grenoble, France), and the Insulet Omnipod 5 (Insulet, Billerica, MA, USA) – are deemed "hybrid" since they require patient intervention to counteract meals and exercise. Insulin boluses in hybrid artificial pancreas effectively reduce postprandial glucose excursions, but subjects need to timely provide an accurate estimation of the ingested carbohydrate to the system. This estimation is challenging for them; estimation errors [11], bolusing delays [12], or omissions [13] frequently degrade the performance achieved by the system. Hybrid artificial pancreas systems usually modify glucose reference or basal profile to reduce the impact of exercise, which requires subjects to announce exercise time or intensity even with anticipation [7].

Several alternatives to meal and exercise control exist in the literature. Meal detection is a popular approach to determine the meal occurrence and increase the aggressiveness against the glucose rise by delivering boluses [14, 15] or retuning the controller [16]. Other approaches rely on disturbance observer-based control [17, 18], robust control techniques [19, 20], model-predictive control [21] or multi-hormonal systems [22]. Many systems apply open-loop-like strategies such as basal reduction or rescue suggestions after detecting the exercise to handle unannounced exercise events [2]. For ex-

ample, Sevil *et al.* [23] detect exercise with accelerometry measurements or Garcia-Tirado *et al.* [8] anticipate it using multi-stage predictions fed with subject historical patterns. Multi-hormonal systems, namely based on glucagon, also have satisfactorily performed against unannounced exercise bouts [24].

Our research group has developed a hybrid artificial pancreas controller, the SAFE-AP [25, 26], which achieved promising results in postprandial control [27]. Ramkissoon *et al.* [28] and Beneyto *et al.* [26] added carbohydrate suggestions to cope with unannounced exercise events – the latter with positive results in clinical trials [29] – but both proposals still need meal announcements. In addition, Sala-Mira *et al.* [30] proposed a meal-detector-based control to remove the meal announcement in the SAFE-AP, but without considering exercise.

This article proposes an add-on module based on an internal model control (IMC, [31]) that eliminates meal and exercise announcements from any hybrid controller that includes some restrictions of the insulin-on board. The module is implemented in the SAFE-AP described above, but any other hybrid artificial pancreas with insulin-on-board restrictions could be used. Lastly, the complete system is validated with the UVA/Padova simulator.

The article is organized as follows: Section 2 describes the proposed add-on module and its tuning and validation procedure. Section 3 presents and discusses the results of the in-silico validation. Finally, Section 4 closes the article with some conclusions and limitations.

## 2. Materials and Methods

The design of any control algorithm embedded in a hybrid artificial pancreas system (henceforth denoted as "main controller") considers that the user will inform the system about meal intake and exercise. In the absence of subject announcements, the main controller will likely perform unsatisfactorily. Figure 1 illustrates a module (see blocks in orange) that replaces those announcements with only minor modifications in the main controller once plugged into it.

The module implements an internal model control loop (IMC) [32] that calculates a "virtual" signal $u_{IMC}(t)$, compensating for the discrepancy between the actual output and an output estimated by a nominal model. Then, a switching logic decomposes this "virtual" signal in a bolus-like insulin infusion ($u_{ins}(t)$) and rescue carbohydrates suggestions ($u_{resc}(t)$) to compensate for hyperglycemia and hypoglycemia, respectively. The switching logic also makes the tolerated insulin-on-board more restrictive after suggesting a rescue carbohydrate intake.

The modification of the tolerated insulin-on-board is the only change the proposed module applies to the internal parameters of the main controller. Most of the hybrid systems constrain the insulin-on-board through gains [33, 34, 35] or thresholds [36, 37, 38]; hence the change of the main controller is immediate. In this article, the main controller implements the SAFE-AP controller [25, 26, 39]. This controller consists of a PID controller with insulin feedback that inhibits the plasma insulin [40] and a safety layer based on a sliding mode reference conditioning that encloses the insulin-on-board below an upper limit [25].

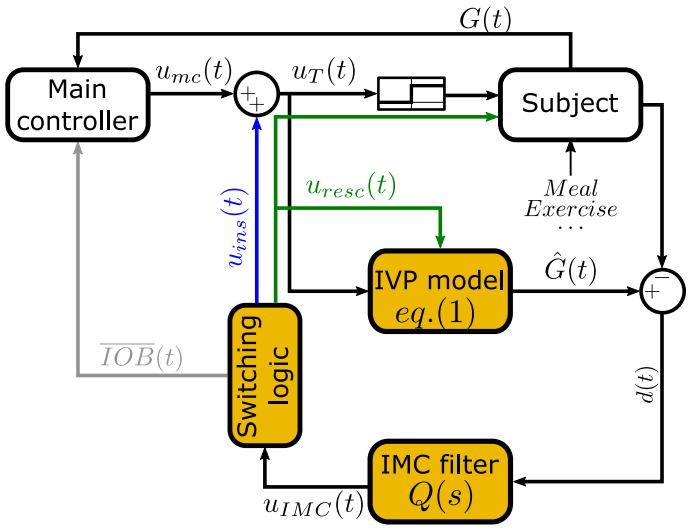


Figure 1: **Overview of the proposed controller**. Blocks with orange background represent the proposed add-on module: an Internal Model Control (IMC) loop (IVP and IMC filter) with a non-linear logic (Switching logic). The add-on module provides three actions: insulin (blue), rescue carbohydrates (dark green), and maximum insulin-on-board (IOB) limit command (grey). Negative values for the total control action, $u_T(t)$, were not allowed. *Notation:* IVP (Identifiable Virtual Patient model).

The following subsections detail the internal model, the switching logic, the controller tuning, and the evaluation.

### *2.1. Output disturbance compensation through Internal Model Control*

#### *2.1.1. Identifiable virtual patient model*

The IMC loop requires a glucose-insulin model (Block "IVP model" in Figure 1). Among the several control-oriented models presented in the literature [41], the Identifiable Virtual Patient (IVP) [42] was selected because of its structural simplicity and physiological interpretability. The equations of

the model are defined as follows,

$$\dot{I}_{SC}(t) = -\frac{1}{\tau_1} I_{SC}(t) + \frac{\kappa}{\tau_1 C_I} u_T(t) \tag{1a}$$

$$\dot{I}_P(t) = -\frac{1}{\tau_2} I_P(t) + \frac{1}{\tau_2} I_{SC}(t) \tag{1b}$$

$$\dot{I}_{EFF}(t) = -p_2 I_{EFF}(t) + p_2 S_I I_P(t) \tag{1c}$$

$$\dot{d_1}(t) = A_g^{resc} \cdot u_{resc}(t) - \frac{d_1(t)}{\tau_{resc}} \tag{1d}$$

$$\dot{d_2}(t) = \frac{1}{\tau_{resc}} \left( d_1(t) - d_2(t) \right) \tag{1e}$$

$$\dot{G}(t) = -GEZI \cdot G(t) - I_{EFF}(t) \cdot G(t) + \tag{1f}$$
$$+ EGP + \frac{d_2(t)}{V_g \tau_{resc}}$$

where $I_{SC}(t)$ and $I_P(t)$ are the subcutaneous and plasma insulin concentrations ($\mu$U/mL), respectively. State $I_{EFF}(t)$ represents the insulin effect (min$^{-1}$), and $G(t)$ is the plasma glucose concentration (mg/dL). The known inputs of the model are the subcutaneous insulin infusion $u_T(t)$ ($\mu$U/min) and the rescue carbohydrate suggestion $u_{resc}(t)$ (mg/min). Any other factor affecting glucose (meals and exercise among others) will correspond to output disturbances. A two-compartment model [43], with the glucose masses (mg) $d_1(t)$, $d_2(t)$ as states, models the rescue carbohydrates absorption. The parameters $\tau_1$ and $\tau_2$ (min) stand for time constants related to insulin absorption, transport, and clearance. . Parameter $p_2$ is the kinetic rate for insulin action (min$^{-1}$) and $V_g$ is the glucose distribution volume (dL). Parameter $C_I$ denotes the insulin clearance gain (mL/min), $S_I$ represents the insulin sensitivity (mL/$\mu$U), $EGP$ is the hepatic glucose production (mg/dL/min), $GEZI$ corresponds to the extrapolation of the glucose effectiveness at zero insulin (min$^{-1}$). Parameter $\tau_{resc}$ is the time to the peak absorption of the

rescue carbohydrate, and $A_g^{resc}$ is the carbohydrate bioavailability [43]. Finally, $\kappa = 60 \cdot 10^{-6}$ is a factor that converts the units of $u_T(t)$ from $\mu$U/min (units of the original model [42]) into U/h.

The parameters of the model (1) were identified from the 10 virtual adults of the academic version of the UVa/Padova simulator [44] since the controller was evaluated with this cohort (Section 2.4). Table 1 includes the identified parameters. The synthetic dataset for identification corresponds to a 2-week basal-bolus therapy of 3 daily meals. Populational values were considered for the absorption dynamics of rescue carbohydrates, and thus parameters in equations (1d)–(1e) were excluded from the identification process. For the identification of the rest of the model parameters, an additional meal model was considered to match clinical data (including meals). However, it must be remarked that this meal model was not part of the IMC controller since meals are unannounced, and thus, they are treated as output disturbances. The meal absorption model matches the structure of (1d)–(1e) but with different signals and parameters involved, e.g., larger doses, longer time constants, etc. The identification process used information available in practical settings (CGM reading, insulin infusion, meal dose, and mealtime). Identifiability issues – such as parameter correlation – were handled by selecting the parameters according to the structural identifiability [45], the global sensitivity [46], and the collinearity index [46] (see [47] for a similar approach).

*2.1.2. Internal model control filter*

The IMC loop compares the output of the IVP model ($\hat{G}(t)$) and the CGM reading ($G(t)$) to form the disturbance term $d(t)$, i.e., $d(t) = \hat{G}(t) -$

| Subject | $EGP$ (mg/dL/min) | $SI$ (mL/$\mu$U/min) | $Vg$ (dL) | $p_2$ (1/min) |
|---|---|---|---|---|
| 1 | 1.32 | $5.17 \cdot 10^{-4}$ | $2.35 \cdot 10^{2}$ | $2.53 \cdot 10^{-3}$ |
| 2 | 1.20 | $4.24 \cdot 10^{-4}$ | $2.48 \cdot 10^{2}$ | $4.08 \cdot 10^{-2}$ |
| 3 | 1.05 | $3.35 \cdot 10^{-4}$ | $1.85 \cdot 10^{2}$ | $2.03 \cdot 10^{-3}$ |
| 4 | 1.49 | $7.23 \cdot 10^{-4}$ | $2.9 \cdot 10^{2}$ | $3.39 \cdot 10^{-3}$ |
| 5 | 0.762 | $2.52 \cdot 10^{-4}$ | $5.81 \cdot 10^{2}$ | $1.12 \cdot 10^{-2}$ |
| 6 | 0.925 | $2.43 \cdot 10^{-4}$ | $1.83 \cdot 10^{2}$ | $4.08 \cdot 10^{-2}$ |
| 7 | 0.916 | $2.84 \cdot 10^{-4}$ | $2.54 \cdot 10^{2}$ | $2.03 \cdot 10^{-3}$ |
| 8 | 0.925 | $2.39 \cdot 10^{-4}$ | $4.57 \cdot 10^{2}$ | $6.9 \cdot 10^{-3}$ |
| 9 | 0.699 | $3.26 \cdot 10^{-4}$ | $2.77 \cdot 10^{2}$ | $4.08 \cdot 10^{-2}$ |
| 10 | 1.53 | $6.03 \cdot 10^{-4}$ | $2.99 \cdot 10^{2}$ | $6.01 \cdot 10^{-3}$ |

| *Populational* | $A_g^{resc}$ (unitless) | $CI$ (mL/min) | $GEZI$ (1/min) | $\tau_1$ (min) |
|---|---|---|---|---|
| | 0.900 | $1.22 \cdot 10^{3}$ | $2.35 \cdot 10^{-3}$ | 74.3 |
| | $\tau_2$ (min) | $\tau_{resc}$ (min) | $A_g^{meal}$ (unitless) | $\tau_{meal}$ (min) |
| | 45.4 | 20.0 | 0.800 | 40.0 |

Table 1: **Control model parameters corresponding to the virtual adults in UVa/Padova simulator.** The first column represents the subject identifier in the simulator. Parameters $EGP$, $SI$, $Vg$, and $p_2$ resulted from optimization. Parameters $CI$, $GEZI$, $\tau_1$, and $\tau_2$ are populational values and correspond to the average of the values in [42]. Parameters $A_g^{resc}$ and $\tau_{resc}$ were chosen to represent a fast-acting carbohydrate rescue; they are populational values too. Meal model parameters ($A_g^{meal}$ and $\tau_{meal}$) were retrieved from [43]. Remark that this meal model was only considered for identification purposes; the IMC controller did not include it since meals were unannounced.

$G(t)$ (see Figure 1). Then, the IMC filter $Q(s)$ generates a "virtual" signal $u_{IMC}(t)$ (in insulin units) that mitigates the effect of $d(t)$ on the output. The term $d(t)$ includes everything not modeled by the IVP model: external disturbances, such as the effect of meal intakes and exercise events, and internal disturbances, such as parametric uncertainty in insulin sensitivity or absorption. Therefore, reducing the effect of $d(t)$ on the output will also attenuate all these disturbances. The IMC filter, $Q(s)$, was selected as in the two-degree-of-freedom IMC [48, 32]:

$$Q(s) = \frac{u_{IMC}(s)}{d(s)} = F(s) \cdot H^{-1}(s) \tag{2}$$

where $s$ is the Laplace variable. $H(s)$ is the linearization of the model (1) (for $u_{resc}(t) = 0$, i.e., the linearized effect of insulin infusion on glucose when $d_1(0) = d_2(0) = 0$) given by

$$H(s) := \frac{G(s)}{u_T(s)} = \frac{S_I G_0^2}{C_I EGP \left(\frac{1}{p_2}s + 1\right)(\tau_1 s + 1)(\tau_2 s + 1)\left(\frac{G_0}{EGP}s + 1\right)} \tag{3}$$

where $G_0$ is the steady-state glucose value reached for the patient's basal insulin infusion.

The filter $F(s)$ is defined as:

$$F(s) = \frac{k}{(\tau s + 1)^5} \tag{4}$$

where $k$ is the gain of the filter (see Section 2.3 for its tuning). The order of the filter is set to 5 for $Q(s)$ to be a strictly proper transfer function when inverting $H(s)$, which is of order 4. The time constant $\tau$ determines the aggressiveness of the filter. Meal intakes and exercise strongly impact plasma

glucose in the short term, but they fade by their dynamics. In addition, due to absorption and measurement lags, the signal $d(t)$ will acknowledge the onset of actual disturbances (e.g., meals, exercise, etc.) with a delay. If $\tau$ is set to a high value, the peak of $u_{IMC}(t)$ will occur much after the disturbance peak; hence reducing the disturbance effect by the filter will be negligible and even counterproductive (e.g., in postprandial control, delayed insulin may lead to hypoglycemia). The filter must quickly react against any deviation in $d(t)$ to reduce the effect of disturbances on glucose. For this reason, $\tau$ is set heuristically to $\tau = 10\,\text{min}$ through exhaustive simulations; this is a low value close to the CGM reading rate (usually, 5 min).

### *2.2. Switching of control actions*

The time constant $\tau$ is set to a low value to counteract the insulin absorption delay by infusing a large amount of insulin in a short time. However, this aggressive tuning amplifies measurement noise, leading to an oscillatory signal $u_{IMC}(t)$ (see Figure 2). The negative values of $u_{IMC}(t)$ would compensate for the positive ones, given the low-pass-filter nature of the glucose-insulin system that avoids transferring this measurement noise effect to the output. However, negative values for insulin are not possible since insulin cannot be removed exogenously. If $u_{IMC}(t)$ were delivered without the negative values would cause an insulin over-delivery, lowering the glucose and even leading to hypoglycemia. Thus, the first goal of the switching logic is to ensure that the proposed loop only applies a control action after a disturbance by removing from $u_{IMC}(t)$ the oscillations caused by measurement noise.

The switching logic also adequates the type of control action to the effect of disturbance on the glucose. Insulin is suitable to compensate for the glu-

cose rise following a meal. However, aerobic low-to-moderate exercise usually leads to a glucose drop and, eventually, hypoglycemia [9], which is unlikely to be compensated with only an insulin reduction [8]. To compensate for glucose drop – usually related to exercise and insulin overdoses within the postprandial period – the switching logic reduces the tolerated insulin-on-board and suggests rescue carbohydrates to the subject. Therefore, the second goal of the switching logic is to convert the "virtual" signal $u_{IMC}(t)$ into three feedforward actions: insulin infusion, rescue carbohydrate suggestion, and insulin-on-board reduction.

*2.2.1. Hyperglycemia compensation*

The proposed loop compensates for a glucose rise with the insulin infusion $u_{ins}(t)$ (Figure 1) that follows a three-phase logic (Figure 2):

1. *Dead-zone.* The insulin $u_{ins}(t)$ is set to 0 if $u_{IMC}(t)$ is lower than a positive threshold $th_{ins}$ to avoid an insulin overdose due to measurement noise amplification in $u_{IMC}(t)$.
2. *Glucose rise mitigation.* Meal ingestion will likely lead to a glucose rise demanding an $u_{IMC}(t)$ that overpasses $th_{ins}$. To compensate for it, $u_{ins}(t)$ matches $u_{IMC}(t)$ until it reaches an upper saturation threshold $th_{sat}$, set to avoid overdosing.
3. *Later hypoglycemia prevention.* Against a glucose rise, the IMC filter reacts first with a positive peak (above phase), but then it will have a negative insulin peak (see the green areas in Figure 2). If $u_{IMC}(t)$ is higher than $th_{resc}$, $u_{ins}(t)$ will equate $u_{IMC}(t)$ to subtract insulin from the main controller, hence avoiding overdosing and the likely related hypoglycemia. If $u_{IMC}(t)$ overpasses $th_{res}$, reducing the insulin from

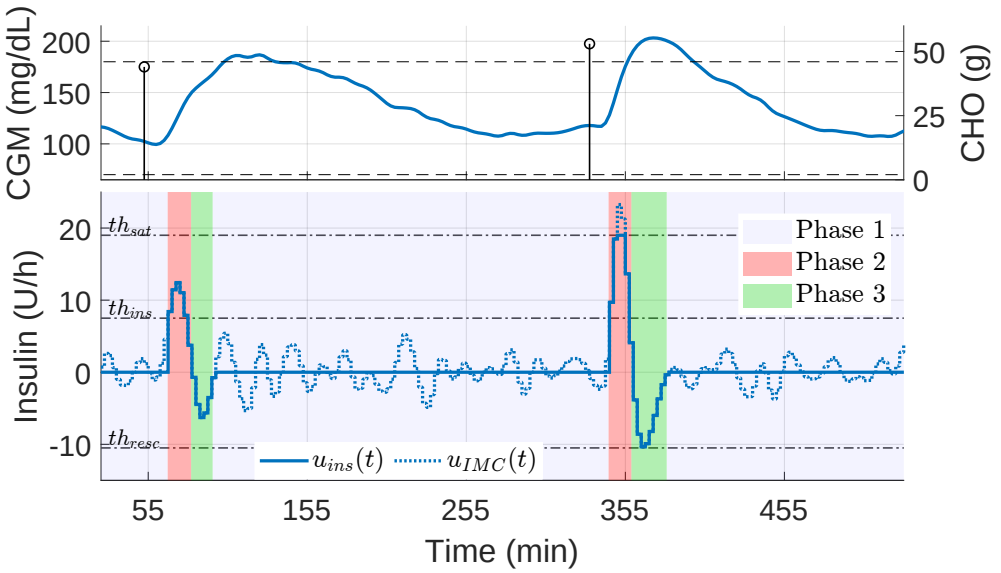


Figure 2: **Control logic to compensate for meals**. The switching logic processes the "virtual" action $u_{IMC}(t)$ in three phases: dead-zone (Phase 1), glucose rise mitigation (Phase 2), and later hypoglycemia prevention (Phase 3). It results in the insulin infusion $u_{ins}(t)$ added to the main controller. Parameters $th_{ins}$, $th_{sat}$, and $th_{resc}$ are, respectively, the thresholds to inhibit $u_{IMC}(t)$, saturate it, or convert it into rescue carbohydrates suggestions, respectively. Note that $u_{ins}(t)$ was allowed to be negative (Phase 3 of Section 2.2.1) to reduce the insulin infusion of the main controller ($u_{mc}(t)$). However, $u_{mc}(t) + u_{ins}(t)$ will be saturated to 0 if $u_{mc}(t) < u_{ins}(t)$.

the main controller may be insufficient. Therefore, the negative-valued insulin is converted into rescue carbohydrates suggestions ($u_{resc}$, see Section 2.2.2), and $u_{ins}(t)$ zeroed to avoid coupling both types of control actions.

### *2.2.2. Hypoglycemia mitigation*

The IMC loop reacts against hypoglycemia with a negative $u_{IMC}(t)$. The switching logic module converts the "negative insulin" into rescue carbohy-

drate suggestions (see around 200 min in Figure 3) to mitigate the hypoglycemia. To this end, first, a "virtual" unquantized carbohydrate signal, $u_{int}(t)$, is calculated by integrating $u_{IMC}(t)$ in a sliding window of length $t_w$ ($t_w = 60\,\text{min}$) as follows:

$$u^*_{IMC}(t) = \begin{cases} u_{IMC}(t) & \text{if} \quad u_{IMC}(t) \leq th_{resc} \\ 0 & \text{otherwise} \end{cases} \tag{5}$$

$$\begin{aligned} u_{int}(t) = -k_{resc} \int_{t-t_w}^{t} u^*_{IMC}(\tau) W(\tau) d\tau - \\ - \int_{t-t_w-T_s}^{t-T_s} u_{resc}(\tau) W(\tau) d\tau \end{aligned} \tag{6}$$

where $T_s$ is the sampling time. The first integral in (6) accumulates the "negative insulin" and transforms it into carbohydrates units (g) through the gain $k_{resc}$, similarly to [28]. Noise or unimportant glucose drops may lead to small negative values in $u_{IMC}(t)$, i.e., if $-th_{resc} \leq u_{IMC}(t) \leq 0$. To avoid suggesting rescue carbohydrates when insulin inhibition may suffice (as in Phase 3 of Section 2.2.1), the first integral in (6) includes the signal $u^*_{IMC}(t)$ instead of $u_{IMC}(t)$. In addition, the forgetting factor $W(t)$ attenuates the earlier values of $u^*_{IMC}(t)$ in the sliding window. $W(t)$ is given by:

$$W(t^*) = 0.1353 \cdot e^{t^*/30} \tag{7}$$

for $t^* \in [t - t_w,\, t]$ where $t$ refers to the current time and $t - t_w$ the beginning of the sliding window (when the earliest value of $u^*_{IMC}(t)$ is considered). The second integral in (6) subtracts the rescue carbohydrates suggested within the sliding window to avoid increasing $u_{int}(t)$.

The "virtual" carbohydrate signal, $u_{int}(t)$, must be quantized for user convenience. The quantized rescue signal, $u_{resc}(t)$, follows the next logic:

$$u_{resc}(t) = \begin{cases} \left\lfloor \frac{u_{int}(t)}{15} \right\rceil \cdot 15 & \text{if } u_{int}(t) \geq 7.5 \,\text{and} \\ & \quad G^*(t) \leq 70 \,\text{and} \\ & \quad \Delta t_{resc} > 15 \\ 15 & \text{if } CGM(t) \leq 70 \,\text{and} \\ & \quad G^*(t) \leq 54 \,\text{and} \\ & \quad \Delta t_{resc} > 15 \\ 0 & \text{otherwise} \end{cases} \tag{8}$$

where $\lfloor \cdot \rceil$ denotes the nearest integer operator and $\Delta t_{resc}$, the elapsed time between two consecutive rescue carbohydrate suggestions (in min). $G^*(t)$ is the 30-min ahead glucose prediction (in mg/dL) computed with the following linear extrapolation:

$$G^*(t) = CGM(t) + 30 \cdot \frac{dCGM(t)}{dt} \tag{9}$$

According to (8), the controller suggests rescue carbohydrates in two situations:

- *When the system predicts a moderate hypoglycemia risk and the accumulated rescue carbohydrates are large enough.* If $u_{int}(t)$ halves the minimum rescue dose – as implemented in [24, 26] – the algorithm calculates a rescue carbohydrate suggestion by approximating $u_{int}(t)$ to the nearest multiple of 15 g since available commercial glucose supplements usually contain 15 g, e.g., Dex4 (Can-Am Care, Alpharetta,

GA, USA), Glutose15 (Paddock Laboratories, Minneapolis, MN, USA), TruePlus (Trividia Health, Fort Lauderdale, FL, USA), etc. If the predicted glucose is outside hypoglycemia risk, the system will not suggest a rescue carbohydrate even though $u_{int}(t) \geq 7.5$ (see the orange squares in Figure 3).

- *When the subject is in moderate hypoglycemia, and the glucose tends to a severe hypoglycemia.* Here, the system suggests a 15-g rescue regardless of the value of $u_{int}(t)$.

The algorithm considers a minimum elapsed time of 15 min between rescue carbohydrates suggestions to avoid frequent recommendations.

Since the exercise impacts the insulin sensitivity even after the exercise event, the switching logic also reduces the insulin-on-board limitation of the main controller to 70% of its nominal value and zeroes $u_{ins}(t)$ within the 3 h following the last rescue carbohydrate suggestion (see the red area in Figure 3). Reducing the insulin-on-board is a common practice in the literature to control exercise [9, 26]. The system restores the nominal values of insulin-on-board limitation and $u_{ins}(t)$ whenever a risk of hyperglycemia exists: when $CGM(t) \geq 140\,\text{mg/dL}$ and $G^*(t) \geq 180\,\text{mg/dL}$.

### *2.3. Optimization-based controller tuning*

The proposed controller has five parameters requiring an individual tuning for the 10 virtual adults in the simulator: the gain of $F(s)$ ($k_{ins}$), the gain factor converting insulin into carbohydrates ($k_{resc}$), and the three thresholds of the switching logic ($th_{ins}$, $th_{sat}$, and $th_{resc}$).

In this section, the parameters are tuned by optimization to provide a common framework for individualizing parameters among the virtual adults (Section 2.3.1). However, the optimization procedure might be unfeasible for a practical setting (e.g., a clinical trial). Therefore, an alternative tuning only relying on open-loop therapy parameters is also proposed in this section (Section 2.3.2).

### *2.3.1. Optimization setting*

For each subject, the worst-case within 12 simulations of the same virtual adult is minimized. The simulations included different sources of variability (e.g., sensor noise, circadian changes in insulin sensitivity, variability in meal and insulin absorption); the random numbers used to create the variability were different among simulations. Each simulation consisted of a 7-day ($T_{sim} = 10080\,\text{min}$) scenario with 3 daily meals and 1 daily exercise session.

The cost applied to each simulation is defined as:

$$J_{sim} := J_{WAIR} + J_C \tag{10}$$

This cost penalizes the weighted areas in risk ($J_{WAIR}$) and constrains the magnitude or shape of the control actions ($J_C$). The weighted areas in risk consider the areas of the CGM exceeding the thresholds 54, 70, 180, and 250 as follows:

$$
\begin{aligned}
J_{WAIR} = a_{uu} \cdot \int_0^{Tsim} (G_{uu}(\tau) - 250)\, d\tau + \\
+ a_u \cdot \int_0^{Tsim} (G_u(\tau) - 180)\, d\tau + \\
+ a_l \cdot \int_0^{Tsim} (70 - G_l(\tau))\, d\tau + \\
+ a_{ll} \cdot \int_0^{Tsim} (54 - G_{ll}(\tau))\, d\tau + \\
+ a_{resc} \cdot \int_0^{Tsim} (G_{resc}(\tau) - 140)\, d\tau
\end{aligned}
\tag{11}
$$

where the scalars $a_{uu} = 175$, $a_u = 1$, $a_l = 5000$, $a_{ll} = 10000$, $a_{resc} = 50$ are the weights. The weights above were tuned so that the areas in hypoglycemia cost more than those in hyperglycemia. This flexibility in configuring the optimal performance is not possible in other approaches that rely on standard metrics to define the cost [49]. All the integrals were calculated using the trapezoidal rule. Signals $G_{uu}(t)$, $G_u(t)$, $G_l(t)$, $G_{ll}(t)$ in (11) correspond to the CGM after being saturated to the enclosing thresholds as follows:

$$G_{uu}(t) := \begin{cases} 250 & \text{if } CGM(t) \leq 250 \\ CGM(t) & \text{otherwise} \end{cases} \tag{12}$$

$$G_{u}(t) := \begin{cases} 180 & \text{if } CGM(t) \leq 180 \\ 250 & \text{if } CGM(t) > 250 \\ CGM(t) & \text{otherwise} \end{cases} \tag{13}$$

$$G_{l}(t) := \begin{cases} 54 & \text{if } CGM(t) < 54 \\ 70 & \text{if } CGM(t) \geq 70 \\ CGM(t) & \text{otherwise} \end{cases} \tag{14}$$

$$G_{ll}(t) := \begin{cases} 54 & \text{if } CGM(t) \geq 54 \\ CGM(t) & \text{otherwise} \end{cases} \tag{15}$$

An insulin overdose might cause a glucose drop that the controller would compensate with rescue carbohydrates suggestions. The last addend of expression (11) weights the glucose rebound after rescue carbohydrate suggestion time to better coordinate rescue carbohydrates suggestions and insulin doses. Signal $G_{resc}(t)$ represents the value of the CGM that overpasses 140 mg/dL in the first 3 h after rescue carbohydrate suggestions. If a meal occurred before the 3 h, $G_{resc}(t)$ was calculated until mealtime as defined in:

$$G_{resc}(t) = \begin{cases} CGM(t) \quad \text{if} \quad (CGM(t) \geq 140) \\ \qquad \text{and } t \in [t_{resc}, \min(t_{resc} + 3\,\text{h}, t_{meal})] \\ 140 \quad \text{otherwise} \end{cases} \tag{16}$$

where $t_{resc}$ and $t_{meal}$ denote the rescue carbohydrates and meals times, respectively. Mealtimes were available to define the cost function but were unknown to the controller.

The cost $J_C$ penalizes the number of times the IMC activates the insulin mode (Phase 2 of Figure 2) for $u_{ins}(t)$ to behave like a bolus (being active for a short time with large insulin doses). In the absence of this penalization, the optimizer usually converged to a bang-bang insulin delivery, which increased the risk of delayed action and, ultimately, hypoglycemia. The cost $J_C$ also constrains the size of rescue carbohydrates. To reduce the risk of compensating for insulin overdosing with rescue carbohydrates, the carbohydrate suggestions followed by meals (meal rescue carbohydrates) were weighted more than those followed by exercise sessions (exercise rescue carbohydrates). For the exercise-related rescue carbohydrates, the average rescue size per exercise event was limited to 45 g. The expression of $J_C$ is the following:

$$\begin{aligned} J_C = b_{act} \cdot \max\left(\frac{n_{imc\_act}}{n_{meal}} - 1, 0\right) + \\ + \quad b_{meal\_resc} \cdot \sum_{i=1}^{n_{meal\_resc}} meal\_resc_i + \\ + \quad b_{ex\_resc} \cdot \max\left(\frac{\sum_{i=1}^{n_{ex\_resc}} ex\_resc_i}{45\, n_{ex\_sessions}} - 1, 0\right) \end{aligned} \tag{17}$$

where $b_{act} = 1400$, $b_{meal\_resc} = 15000$, and $b_{ex\_resc} = 4500$ are weights. Terms $n_{imc\_act}$, $n_{meal\_resc}$, $n_{ex\_resc}$, $n_{ex\_session}$ denote the number of times the IMC enters Phase 2, the number of meal-related rescue carbohydrates, the number of exercise-related rescue carbohydrates, and the number of exercise sessions, respectively. $meal\_resc_i$ represents the meal rescue sizes (from

$i = 1$ to $i = n_{meal\_resc}$) and $meal\_ex_i$ the exercise rescue sizes (from $i = 1$ to $i = n_{ex\_resc}$)

The min-max problem was solved with the Covariance Matrix - Adaptation Evolution Strategy (CMA-ES) algorithm, a black-box search optimizer suitable for non-linear or non-convex problems [50]. Table 2 includes the starting values and the bounds of the parameters. To reduce the computational time, the optimization was executed in the computing cluster of the Politechnical University of Valencia (Universitat Politècnica de València, València, Spain) using 12 cores of 3 GB [51]. Note that this optimization process is only required to tune the algorithm. Once the control parameters are obtained, the module can be executed in real-time without any optimization procedure.

| | Initial value | Lower limit | Upper limit |
|---|---|---|---|
| $k_{ins}$ (-) | 0.5 | 0.01 | 1 |
| $th_{ins}$ (U/h) | 5 | 1 | 30 |
| $th_{sat}$ (U/h) | 10 | 1 | 30 |
| $th_{resc}$ (U/h) | 1 | 0.05 | 5 |
| $k_{resc}$ (g/U/h) | 0.1 | 0.0005 | 0.5 |

Table 2: **Initial values and bounds of the parameters in the optimization**

### *2.3.2. Regression with open-loop parameters*

The method presented in Section 2.3.1 to tune the controllers is only feasible for in-silico studies. To provide a starting tuning for a clinical trial, the optimal parameters were related to standard parameters of the open-loop therapy [52]: the weight ($BW$, in kg), the total daily insulin ($TDI$, in U), the basal insulin ($u_b$, in U/h), the carbohydrate-to-insulin ratio ($CR$, in g/U), and the correction factor ($CF$, in mg/dL/U) [53]. The values were available in the UVa/Padova simulator. For each optimal parameter, a relation to open-loop parameters was found as follows:

1. The 80 linear models that fit the corresponding optimal parameter with the lowest root sum of squares were selected. Models had up to 8 coefficients, including pairwise interactions of the open-loop parameters. The selection was performed with the function `regsubset` [54] of the R software [55].
2. To mitigate the risk of overfitting, the selected models were fitted using leave-one-out cross-validation [56].
3. The final model was the model with the lowest number of coefficients that resulted in a low cross-validation root-mean-squared error and satisfied the diagnosis assumptions (normality and homoscedasticity of the residuals).

## *2.4. Validation setting*

The proposed add-on module was implemented in an extended version of the UVA/Padova simulator for validation purposes. The simulator emulates the 5-min sampling time of the CGM; hence the add-on module must be

implemented in discrete time. For the implementation, the model in (1) was discretized with Euler approximation using a sampling period of 5 min ($T_s = 5\,\text{min}$). The filter $Q(s)$ in (2) and the integral in (6) were discretized using the Tustin approximation [57], also with $T_s = 5\,\text{min}$.

The validation targets three purposes: 1) to determine whether the regression-based tuning maintains the performance of the optimal tuning, 2) to assess the controller against meals, and 3) to assess the controller against meals and exercise. The details of the validation are given in the following subsections.

*2.4.1. Validation of the regression-based tuning*

The fit of the regression model to the corresponding optimal parameter was assessed with the coefficient of determination $R^2$ and the root-mean-squared error of the cross-validation ($RMSE_{loocv}$).

To study if the regression-based tuning degraded the performance of the optimal tuning, glucose percentage time-related metrics were compared (the %time in range, the %time in hyperglycemia, and the %time in hypoglycemia). To this end, both tunings were simulated for the 10 virtual adults of the UVa/Padova simulator academic version [44]. The simulation consisted of a 30-day scenario including 3 daily meals – with random sizes and timing: 49.5 [33.0, 55.0] g for breakfast at 6.92 [6.75, 7.08] h , 81.0 [72.0, 93.0] g at 13.75 [13.58, 14.17] h for lunch, and 64 [54, 79] g at 20.9 [20.8, 21.1] h for dinner, median [interquartile range]) – and 1 daily exercise session. Exercise effect on glucose was simulated through a variation of insulin sensitivity [58]. This exercise model corresponds to an aerobic exercise of 60 min at 50% of $VO_2$, approximately [58]. The exercise time was set up to 240 min after one meal of the day – 12 exercise events after breakfast, 11 after

lunch, and 7 after dinner – following a uniform distribution. Exercise events beyond midnight were avoided.

The simulation also included CGM noise (the built-in sensor model *dexcom25*) and multiple sources of parametric variability added to the educational version of the simulator such as one-day period sinusoidal-type insulin sensitivity variation with random amplitude and phase, variation of subcutaneous insulin absorption rate at each meal following a uniform distribution of $\pm 30\%$, or variability of the meal absorption parameters, which nominal values where changed at each meal randomly selecting a parameter set from the ones provided in the simulator in order to emulate ingestion of different meal types.

### *2.4.2. Validation of the performance against meals*

The goal of this validation is to quantize the improvement regarding the main controller without any meal compensation (henceforth denoted as No-Comp) of three controllers with meal compensation: 1) the main controller with the IMC loop, tuned with the regression model (denoted as mIMC), 2) the main controller with the meal-announcement free compensation feature of [30], based on a super-twisting meal detector (referred as MD), and 3) the main controller with meal announcements but considering errors in the estimation of the carbohydrates according to the model in [11] (denoted as Hybrid).

The simulation features – duration, number of subjects, variability, meal size, and timing– were identical to those described in Section 2.4.1, but without considering exercise.

To assess the controllers, apart from the standard metrics proposed in

[59], percentage-time-related metrics within the postprandial period (from mealtime until 3 h after each meal) were calculated. Since the mIMC might compensate for insulin over-delivery with rescue carbohydrates suggestions, the percentage of meals requiring at least one rescue and the mean size of the rescue carbohydrates suggested for those meals were also reported.

### *2.4.3. Validation of the performance against exercise*

This validation assessed the likely benefits of the rescue carbohydrate suggestion feature of the mIMC to counteract exercise-induced hypoglycemias. To this end, the proposed controller mIMC was compared to two insulin-only controllers: 1) the mIMC controller with the rescue carbohydrate suggestion feature deactivated (denoted as NoExComp), and 2) the meal-detector based controller, i.e., MD.

The simulation scenario was identical to the one described in Section 2.4.1. Besides the metrics suggested by [59], the following exercise-related metrics were computed: the %time in hypoglycemia within the exercise period (from the exercise time to 3 h after it), the %time above 140 mg/dL up to 3 h after each rescue, the percentage of exercise events needing at least one rescue carbohydrate, and the mean rescue size suggested for those events.

In the simulations, subjects ingested the suggested carbohydrates in the precise time and size as in [26, 24, 28].

### *2.4.4. Statistic analysis*

Results were analyzed with a regression-based inference approach and Wald 95% confidence intervals [60]. Since all the simulations in the study shared the virtual cohort, the independence condition assumed by linear

models fails. Mixed-effect models can handle the dependency of the virtual subjects in the sample [61]. For each of the analyzed metrics, the following random-intercept mixed-effect model, individualized for each subject, was fitted:

$$y_{sub} = \beta_0 + S_{sub} + \sum_{i=1}^{n_C-1} \beta_i x_i + e_{sub} \tag{18}$$

where $y_{sub}$ is the corresponding metric value for a given subject, *sub*, and $n_C$ is the number of controllers to be compared. $S_{sub}$ is the random intercept, and $e_{sub}$ are the residuals, following both a zero-mean normal distribution [61]. Fixed coefficient $\beta_0$ is the intercept, and coefficients $\beta_i$ can be interpreted as the mean difference regarding the intercept since $x_i$ is a dichotomous dummy variable related to the controller to be compared with the intercept. These coefficients inform about the effect size of the differences between structures, a pece of more valuable information than the significance analysis of P-values [62], especially for in silico analysis where P-values are controversial [63].

The mixed-effect model was fitted with the robust method presented in [64] of the R software [55] to handle the outliers appearing in the data.

## 3. Results and Discussion

### *3.1. Controller tuning*

Table 3 includes the optimal parameters of the controller described in Section 2.3. The related regression equations (Table 4) fit the optimal parameters with a reduced cross-validation root-mean squared error.

Furthermore, the mean difference in the metrics %time in 70–180 mg/dL (0.303%, CI:[−1.30, 1.91]), %time above 180 mg/dL (−0.470%, CI:[−2.29, 1.35]),

| Subject | $k_{ins}$ (-) | $th_{min}$ (U/h) | $th_{max}$ (U/h) | $k_{resc}$ (g/U/h) | $th_{resc}$ (U/h) |
|---|---|---|---|---|---|
| 1 | 0.04 | 4.43 | 9.38 | 0.09 | 0.48 |
| 2 | 0.17 | 1.46 | 14.34 | 0.31 | 0.15 |
| 3 | 0.03 | 1.08 | 13.20 | 0.06 | 0.53 |
| 4 | 0.08 | 5.50 | 12.19 | 0.12 | 0.07 |
| 5 | 0.11 | 3.72 | 25.95 | 0.09 | 0.07 |
| 6 | 0.25 | 7.57 | 19.62 | 0.12 | 2.08 |
| 7 | 0.02 | 5.42 | 10.25 | 0.09 | 0.12 |
| 8 | 0.14 | 6.83 | 15.22 | 0.05 | 2.45 |
| 9 | 0.34 | 2.34 | 8.08 | 0.16 | 0.72 |
| 10 | 0.14 | 9.69 | 15.69 | 0.09 | 0.35 |

Table 3: **Control parameters that resulted from optimization.** The first column represents the virtual adult identifier in the UVa/Padova Simulator. The second, third, and fourth columns include the parameters used for meal compensation, while the remaining columns correspond to the exercise compensation (see Section 2.3).

and %time below 70 mg/dL (0.0576%, CI:[−0.199, 0.315]) are negligible, which indicate that the regression-based tuning preserves the performance achieved by the optimal tuning.

### *3.2. Performance of postprandial control*

The controllers featuring meal compensation (Hybrid, MD, or mIMC) outperform NoComp, as shown in Table 5. The improvement is statistically significant since all the fixed-effect coefficients of Figure 4 and Figure 5 – interpreted as the mean difference of each controller regarding NoComp – are far from zero.

Since the confidence intervals in Figure 4 and Figure 5 overlap among controllers, all the controllers with meal compensation improve to a similar degree the performance of NoComp, with the advantage that the MD and mIMC controllers free subjects from meal announcements.

Figure 6 shows the glucose and insulin traces for 2 of the 30 days of the simulation. Some behavioral differences exist between the controllers. The meal announcement in the hybrid controller improves the early phase of the postprandial with a lower time in hyperglycemia (see bottom panel of Figure 4) and a lower postprandial peak (Figure 6).

The mIMC tends to be more aggressive, allowing a more rapid recovery than the hybrid controller after large meals (see fifth meal in Figure 6). The price to pay to achieve a similar time in range to the hybrid controller, but without announcement, is a steeper glucose drop after the postprandial (Figure 6). In no subject, the glucose drops below 54 mg/dL and the %time below 70 mg/dL never overpasses the 0.5%, which is far from the 4% threshold indicated in the literature [59]. However, since this is an in-silico evaluation,

the results must be interpreted with caution and the module may achieve larger time in hypoglycemia under real-life situations.

Although the rescue suggestion feature plays a role in avoiding hypoglycemia events, its use was sparse: for most of the subjects, the controller did not suggest any rescue; for two of them, the controller only recommended 15 g; and only for the two remaining ones, the controller recommended more than one rescue – 10 and 12 rescues –, always of 15 g.

Finally, the MD achieves a slightly longer time in hyperglycemia than the mIMC (Table 5). Since the MD does not suggest rescues [30], it cannot mitigate the glucose drop. As a result, unlike the mIMC, one virtual subject had severe hypoglycemia.

### *3.3. Performance of exercise control*

The carbohydrate suggestion feature in the mIMC significantly reduces the time in moderate and severe hypoglycemia (Figure 8) compared to when the rescue module is unable (NoExComp). The meal-detector-based controller (MD) performed like NoExComp as concluded from the confidence intervals – they are small and include the 0 (Table 6, Figure 8). Therefore, the flexibility of insulin-only controllers against exercise-induced hypoglycemia is limited.

The mIMC suggested a median of 27.2 g per exercise session to handle the exercise-induced glucose drop (Table 6); this value is coherent with other results of unannounced exercise events in the literature [26, 24, 28]. Even with the additional carbohydrate intake, the controller achieved a time in hyperglycemia similar to the NoExComp (Figure 7). The mIMC increases the CGM mean a 4.28 mg/dL (CI:2.90 – 5.91) mg/dL on average; although

statistically significant, this increase, concerning NoExComp, has a minor relevance from the clinical point of view. The rise in the %time above 140 mg/dL after the rescue carbohydrate suggestion is also permissible (Table 6).

| | NoExComp | MDresc | mIMC |
|---|---|---|---|
| **Overall** | | | |
| Mean CGM (mg/dL) | 138.2 [132.1, 141.7] | 140.6 [138.6, 142.7] | 141.9 [136.5, 146.2] |
| CV (%) | 33.3 [31.4, 34.4] | 30.9 [28.3, 31.6] | 29.6 [27.4, 32.0] |
| $>$ 250 mg/dL | 1.6 [0.8, 2.9] | 2.2 [1.6, 3.6] | 1.6 [1.0, 2.9] |
| $>$ 180 mg/dL | 19.2 [13.5, 21.1] | 19.2 [18.2, 20.6] | 19.8 [13.6, 20.8] |
| 70 – 180 mg/dL | 75.5 [72.7, 81.5] | 80.8 [79.4, 81.8] | 79.6 [77.5, 85.5] |
| $<$ 70 mg/dL | 5.3 [4.5, 6.6] | 0.0 [0.0, 0.0] | 0.9 [0.4, 1.1] |
| $<$ 54 mg/dL | 3.7 [2.2, 4.1] | 0.0 [0.0, 0.0] | 0.0 [0.0, 0.0] |
| Daily insulin (U) | 37.9 [33.0, 40.7] | 38.1 [32.7, 41.1] | 37.7 [33.2, 40.6] |
| Daily CHO (g) | 0.0 [0.0, 0.0] | 50.0 [47.5, 57.6] | 27.5 [23.9, 31.0] |
| **Exercise control** | | | |
| $<$ 70 mg/dL | 38.3 [34.6, 44.1] | 0.0 [0.0, 0.3] | 6.5 [3.0, 8.7] |
| $<$ 54 mg/dL | 27.0 [17.0, 30.4] | 0.0 [0.0, 0.0] | 0.1 [0.0, 0.3] |
| $>$ 140 mg/dL (rescues) | - | 4.3 [3.7, 5.2] | 9.6 [5.6, 12.8] |
| Events needing rescues (%) | 0.0 [0.0, 0.0] | 96.7 [96.7, 96.7] | 96.7 [96.7, 96.7] |
| Mean rescues (g) | - | 48.5 [47.7, 60.2] | 27.2 [23.7, 31.0] |

## 4. Conclusion

This work has proposed an add-on module based on a modified Internal Model Control that removes meal and exercise announcements of a hybrid artificial pancreas. The module was integrated into a PID-based hybrid ar-

tificial pancreas developed previously by our research group. In in silico simulations, the module preserved the %time in range achieved by the hybrid artificial pancreas, considering carbohydrate counting errors, without a relevant increase in the time in hypoglycemia. The rescues suggested by the controller counteracted the exercise-induced hypoglycemia, allowing more flexibility than insulin-only controllers.

Despite the positive results, further studies should be performed. For tuning the module parameters, the regression models were fitted to just 10 subjects – the available adult cohort in the educational version of the simulator – which increases the risk of overfitting. In addition, the latter virtual cohort was also used to validate the proposed module. Although the validation included a different instance of variability, assessing the module with the same virtual cohort used for tuning it may limit the generalization of the method to real patients. In the future, the subject cohort must be expanded to improve the tuning, for example, using recent subject cloning techniques from clinical data [65]. Even though a more extended population was used to fit the regression equations, these equations would only provide an initial tuning; only adapting the parameters would guarantee an acceptable long-term performance against the intra-patient variability.

Moreover, the study only considered low-to-moderate intensity aerobic exercise events, leading to hypoglycemia events. The glycemic impact of the exercise is complex, and depending on its type, intensity, duration, or even the time of the day it occurs, it might lead to a glucose rise [66, 7], requiring a different strategy to handle it.

## Funding

This work was partially supported by: grant PID2019-107722RB-C21 funded by MCIN/AEI/10.13039/501100011033 and grant ACIF/2017/021 funded by the Generalitat Valenciana through FSE funds.

## Conflict of interest statement

None

## Acknowledgments

The authors would like to thank the ASIC (Area de Sistemas de Información y Comunicaciones) for technical access to the computing cluster of the Universitat Politècnica de València.

## References

[1] E. Bekiari, K. Kitsios, H. Thabit, M. Tauschmann, E. Athanasiadou, T. Karagiannis, A.-B. Haidich, R. Hovorka, A. Tsapas, Artificial pancreas treatment for outpatients with type 1 diabetes: systematic review and meta-analysis, BMJ 361 (2018) 1310. doi:10.1136/BMJ.K1310.

[2] C. K. Boughton, R. Hovorka, New closed-loop insulin systems, Diabetologia (feb 2021). doi:10.1007/s00125-021-05391-w.

[3] T. D. C. Group, C. T. Research, The Effect of Intensive Treatment of Diabetes on the Development and Progression of Long-Term Complications in Insulin-Dependent Diabetes Mellitus, New Eng-

land Journal of Medicine 329 (14) (1993) 977–986. doi:10.1056/NEJM199309303291401.

[4] J.-C. Orban, E. Van Obberghen, C. Ichai, Acute Complications of Diabetes, in: Metabolic Disorders and Critically Ill Patients, Springer International Publishing, Cham, 2018, Ch. 15, pp. 341–363. doi:10.1007/978-3-319-64010-5_15.

[5] V. Gingras, N. Taleb, A. Roy-Fleming, L. Legault, R. Rabasa-Lhoret, The challenges of achieving postprandial glucose control using closed-loop systems in patients with type 1 diabetes, Diabetes, Obesity and Metabolism 20 (2) (2018) 245–256. doi:10.1111/dom.13052.

[6] A. E. Fathi, V. Gingras, B. Boulet, A. El Fathi, M. Raef Smaoui, V. Gingras, B. Boulet, A. Haidar, The Artificial Pancreas and Meal Control: An overview of postprandial glucose regulation in type 1 diabetes, IEEE Control Systems 38 (February) (2018) 67–85. doi:10.1109/MCS.2017.2766323.

[7] D. P. Zaharieva, L. H. Messer, B. Paldus, D. N. O'Neal, D. M. Maahs, M. C. Riddell, Glucose Control During Physical Activity and Exercise Using Closed Loop Technology in Adults and Adolescents with Type 1 Diabetes, Canadian Journal of Diabetes 44 (8) (2020) 740–749. doi:10.1016/J.JCJD.2020.06.003.

[8] J. Garcia-Tirado, S. A. Brown, N. Laichuthai, P. Colmegna, C. L. Koravi, B. Ozaslan, J. P. Corbett, C. L. Barnett, M. Pajewski, M. C. Oliveri, H. Myers, M. D. Breton, Anticipation of Historical Exercise

Patterns by a Novel Artificial Pancreas System Reduces Hypoglycemia during and after Moderate-Intensity Physical Activity in People with Type 1 Diabetes, Diabetes Technology and Therapeutics 23 (4) (2021) 277–285. doi:10.1089/dia.2020.0516.

[9] O. Moser, M. C. Riddell, M. L. Eckstein, P. Adolfsson, R. Rabasa-Lhoret, L. van den Boom, P. Gillard, K. Nørgaard, N. S. Oliver, D. P. Zaharieva, T. Battelino, C. de Beaufort, R. M. Bergenstal, B. Buckingham, E. Cengiz, A. Deeb, T. Heise, S. Heller, A. J. Kowalski, L. Leelarathna, C. Mathieu, C. Stettler, M. Tauschmann, H. Thabit, E. G. Wilmot, H. Sourij, C. E. Smart, P. G. Jacobs, R. M. Bracken, J. K. Mader, Glucose management for exercise using continuous glucose monitoring (CGM) and intermittently scanned CGM (isCGM) systems in type 1 diabetes: position statement of the European Association for the Study of Diabetes (EASD) and of the International Society f, Diabetologia 63 (12) (2020) 2501–2520. doi:10.1007/s00125-020-05263-9.

[10] D. A. Domingo-Lopez, G. Lattanzi, L. H. J. Schreiber, E. J. Wallace, R. Wylie, J. O'Sullivan, E. B. Dolan, G. P. Duffy, Medical Devices, Smart Drug Delivery, Wearables and Technology for the treatment of Diabetes Mellitus, Advanced Drug Delivery Reviews (2022) 114280doi:10.1016/j.addr.2022.114280.
URL https://doi.org/10.1016/j.addr.2022.114280https://linkinghub.elsevier.com/retrieve/pii/S0169409X22001703

[11] T. Kawamura, C. Takamura, M. Hirose, T. Hashimoto, T. Higashide, Y. Kashihara, K. Hashimura, H. Shintaku, The factors affecting on

estimation of carbohydrate content of meals in carbohydrate counting, Clinical Pediatric Endocrinology 24 (4) (2015) 153–165. doi:10.1297/cpe.24.153.

[12] C. K. Boughton, S. Hartnell, J. M. Allen, R. Hovorka, The importance of prandial insulin bolus timing with hybrid closed-loop systems, Diabetic Medicine (2019) dme.14116doi:10.1111/dme.14116.

[13] D. Elleri, G. Maltoni, J. M. Allen, M. Nodale, K. Kumareswaran, L. Leelarathna, H. Thabit, K. Caldwell, M. E. Wilinska, P. Calhoun, C. Kollman, D. B. Dunger, R. Hovorka, Safety of closed-loop therapy during reduction or omission of meal boluses in adolescents with type 1 diabetes: A randomized clinical trial, Diabetes, Obesity and Metabolism 16 (11) (2014) 1174–1178. arXiv:NIHMS150003, doi:10.1111/dom.12324.

[14] A. E. Fathi, E. Palisaitis, B. Boulet, L. Legault, A. Haidar, An Unannounced Meal Detection Module for Artificial Pancreas Control Systems, in: 2019 American Control Conference (ACC), Vol. 2019-July, IEEE, 2019, pp. 4130–4135. doi:10.23919/ACC.2019.8814932.

[15] Z. Mahmoudi, F. Cameron, N. K. Poulsen, H. Madsen, B. W. Bequette, J. B. Jørgensen, Sensor-based detection and estimation of meal carbohydrates for people with diabetes, Biomedical Signal Processing and Control 48 (2019) 12–25. doi:10.1016/J.BSPC.2018.09.012.

[16] E. Fushimi, P. Colmegna, H. De Battista, F. Garelli, R. Sánchez-Peña, Artificial Pancreas: Evaluating the ARG Algorithm Without Meal

Announcement, Journal of Diabetes Science and Technology (2019). doi:10.1177/1932296819864585.

[17] R. Sanz, P. Garcia, J.-L. Diez, J. Bondia, Artificial Pancreas System With Unannounced Meals Based on a Disturbance Observer and Feedforward Compensation, IEEE Transactions on Control Systems Technology (2020) 1–7doi:10.1109/TCST.2020.2975147.

[18] P. Abuin, P. S. Rivadeneira, A. Ferramosca, A. H. González, Artificial pancreas under stable pulsatile MPC: Improving the closed-loop performance, Journal of Process Control 92 (2020) 246–260. doi:10.1016/j.jprocont.2020.06.009.

[19] L. Kovacs, G. Eigner, M. Siket, L. Barkai, Control of Diabetes Mellitus by Advanced Robust Control Solution, IEEE Access 4 (2019) 1–1. doi:10.1109/ACCESS.2019.2938267.

[20] E. Ruiz-Velázquez, J. García-Rodríguez, G. Quiroz, R. Femat, Robust $\mu$-synthesis: towards a unified glucose control in adults, adolescents and children with T1DM, Journal of the Franklin Institute (jul 2020). doi:10.1016/j.jfranklin.2020.07.030.

[21] I. Hajizadeh, N. Hobbs, M. Sevil, M. Rashid, M. R. Askari, R. Brandt, A. Cinar, Performance Monitoring , Assessment and Modification of an Adaptive MPC : Automated Insulin Delivery in Diabetes, in: 2020 European Control Conference (ECC), Saint Petersburg, Russia, 2020, pp. 283–288.

[22] D. Majdpour, M. Tsoukas, J.-F. Yale, A. El Fathi, J. Rutkowski, J. Rene, N. Garfield, L. Legault, A. Haidar, Fully Automated Artificial Pancreas for Adults with Type 1 Diabetes using Multiple Hormones: Exploratory Experiments, Canadian Journal of Diabetes (2021) 135938doi:10.1016/j.jcjd.2021.02.002.

[23] M. Sevil, M. Rashid, M. R. Askari, Z. Maloney, I. Hajizadeh, A. Cinar, Detection and Characterization of Physical Activity and Psychological Stress from Wristband Data, Signals 1 (2) (2020) 188–208. doi:10.3390/signals1020011.

[24] V. Moscardó, J. L. Díez, J. Bondia, Parallel Control of an Artificial Pancreas with Coordinated Insulin, Glucagon, and Rescue Carbohydrate Control Actions, Journal of Diabetes Science and Technology 13 (6) (2019) 1026–1034. doi:10.1177/1932296819879093.

[25] A. Revert, F. Garelli, J. Pico, H. De Battista, P. Rossetti, J. Vehi, J. Bondia, Safety Auxiliary Feedback Element for the Artificial Pancreas in Type 1 Diabetes, IEEE Transactions on Biomedical Engineering 60 (8) (2013) 2113–2122. doi:10.1109/TBME.2013.2247602.

[26] A. Beneyto, A. Bertachi, J. Bondia, J. Vehi, A New Blood Glucose Control Scheme for Unannounced Exercise in Type 1 Diabetic Subjects, IEEE Transactions on Control Systems Technology PP (2018) 1–8. doi:10.1109/TCST.2018.2878205.

[27] P. Rossetti, C. Quirós, V. Moscardó, A. Comas, M. Giménez, F. J. Ampudia-Blasco, F. León, E. Montaser, I. Conget, J. Bondia, J. Vehí,

Closed-loop control of postprandial glycemia using an insulin-on-board limitation through continuous action on glucose target, Diabetes Technology & Therapeutics 19 (6) (2017) 355–362. doi:10.1089/dia.2016.0443.

[28] C. M. Ramkissoon, A. Bertachi, A. Beneyto, J. Bondia, J. Vehi, Detection and Control of Unannounced Exercise in the Artificial Pancreas without Additional Physiological Signals, IEEE Journal of Biomedical and Health Informatics 2194 (c) (2019) 1–1. doi:10.1109/JBHI.2019.2898558.

[29] C. Viñals, A. Beneyto, J.-F. Martín-SanJosé, C. Furió-Novejarque, A. Bertachi, J. Bondia, J. Vehi, I. Conget, M. Giménez, C. Viñals -vinals, J.-F. Martín-SanJosé -, A. Bertachi -, J. Vehí, Artificial pancreas with carbohydrate suggestion performance for unannounced and announced exercise in Type 1 Diabetes, The Journal of Clinical Endocrinology & Metabolism (2020). doi:10.1210/clinem/dgaa562/5895273.

[30] I. Sala-Mira, J.-L. Díez, B. Ricarte, J. Bondia, Sliding-mode disturbance observers for an artificial pancreas without meal announcement, Journal of Process Control 78 (2019) 68–77. doi:10.1016/j.jprocont.2019.03.008.

[31] M. Morari, Internal Model Control - Theory and Applications., IFAC Proceedings Series 16 (21) (1984) 1–18. doi:10.1016/s1474-6670(17)64183-1.
URL http://dx.doi.org/10.1016/S1474-6670(17)64183-1

[32] G. Chen, J. Zhang, Z. Zhao, A Two-Degree-of-Freedom IMC Parameters Online Intelligent Tuning Method, in: 2010 International Conference on Computational Aspects of Social Networks, IEEE, 2010, pp. 483–486. doi:10.1109/CASoN.2010.114.

[33] J. L. Ruiz, J. L. Sherr, E. Cengiz, L. Carria, A. Roy, G. Voskanyan, W. V. Tamborlane, S. A. Weinzimer, Effect of insulin feedback on closed-loop glucose control: A crossover study, Journal of Diabetes Science and Technology 6 (5) (2012) 1123–1130. doi:10.1177/193229681200600517.

[34] K. Turksoy, L. Quinn, E. Littlejohn, A. Cinar, Multivariable adaptive identification and control for artificial pancreas systems, IEEE Transactions on Biomedical Engineering 61 (3) (2014) 883–891. arXiv:arXiv:1402.6991v1, doi:10.1109/TBME.2013.2291777.

[35] S. Khodakaramzadeh, Y. Batmani, N. Meskin, Automatic blood glucose control for type 1 diabetes: A trade-off between postprandial hyperglycemia and hypoglycemia, Biomedical Signal Processing and Control 54 (2019) 101603. doi:10.1016/J.BSPC.2019.101603.

[36] C. Ellingsen, E. Dassau, H. Zisser, B. Grosman, M. W. Percival, L. Jovanovič, F. J. Doyle, Safety constraints in an artificial pancreatic $\beta$ cell: An implementation of model predictive control with insulin on board, Journal of Diabetes Science and Technology 3 (3) (2009) 536–544. doi:10.1177/193229680900300319.

[37] R. Hu, C. Li, An Improved PID Algorithm Based on Insulin-on-Board

Estimate for Blood Glucose Control with Type 1 Diabetes, Computational and Mathematical Methods in Medicine 2015 (2015). doi:10.1155/2015/281589.

[38] Y. Batmani, S. Khodakaramzadeh, P. Moradi, Automatic Artificial Pancreas Systems Using an Intelligent Multiple-Model PID Strategy, IEEE Journal of Biomedical and Health Informatics 2194 (c) (2021). doi:10.1109/JBHI.2021.3116376.

[39] I. Sala-Mira, J. Díez, J. Bondia, Insulin limitation in the Artificial Pancreas by Sliding Mode Reference Conditioning and Insulin Feedback: an in silico comparison, IFAC-PapersOnLine 50 (1) (2017) 7743–7748. doi:10.1016/j.ifacol.2017.08.1153.

[40] G. M. Steil, C. C. Palerm, N. Kurtz, G. Voskanyan, A. Roy, S. Paz, F. R. Kandeel, The effect of insulin feedback on closed loop glucose control, Journal of Clinical Endocrinology and Metabolism 96 (5) (2011) 1402–1408. doi:10.1210/jc.2010-2578.

[41] M. E. Wilinska, R. Hovorka, Simulation Models for In-Silico Evaluation of Closed-Loop Insulin Delivery Systems in Type 1 Diabetes, in: V. Marmarelis, G. Mitsis (Eds.), Data-driven Modeling for Diabetes. Lecture Notes in Bioengineering, Springer, Berlin, Heidelberg, 2014, Ch. 6, pp. 131–149. doi:10.1007/978-3-642-54464-4_6.

[42] S. Kanderian, Steil, G. Steil, Identification of Intraday Metabolic Profiles during Closed-Loop Glucose Control in Individuals with Type 1

Diabetes, Journal of Diabetes Science and Technology 3 (5) (2009) 1047–1057. doi:10.1177/193229680900300508.

[43] R. Hovorka, V. Canonico, L. J. Chassin, U. Haueter, M. Massi-Benedetti, M. O. Federici, T. R. Pieber, H. C. Schaller, L. Schaupp, T. Vering, M. E. Wilinska, Nonlinear model predictive control of glucose concentration in subjects with type 1 diabetes, Physiological Measurement 25 (4) (2004) 905–920. doi:10.1088/0967-3334/25/4/010.

[44] C. Dalla Man, F. Micheletto, D. Lv, M. Breton, B. Kovatchev, C. Cobelli, The UVA/PADOVA type 1 diabetes simulator: New features, Journal of Diabetes Science and Technology 8 (1) (2014) 26–34. doi:10.1177/1932296813514502.

[45] O.-T. Chis, J. R. Banga, E. Balsa-Canto, Structural Identifiability of Systems Biology Models: A Critical Comparison of Methods, PLoS ONE 6 (11) (2011) e27755. doi:10.1371/journal.pone.0027755.

[46] R. Brun, P. Reichert, H. R. Künsch, Practical identifiability analysis of large environmental simulation models, Water Resources Research 37 (4) (2001) 1015–1030. doi:10.1029/2000WR900350.

[47] J. Garcia-Tirado, C. Zuluaga-Bedoya, M. D. Breton, Identifiability Analysis of Three Control-Oriented Models for Use in Artificial Pancreas Systems, Journal of Diabetes Science and Technology 12 (5) (2018) 937–952. doi:10.1177/1932296818788873.

[48] N. Abe, K. Seki, H. Kanoh, Two degree of freedom internal model control for single tubular heat exchanger system, in: Proceedings of IEEE

International Symposium on Industrial Electronics, Vol. 1, IEEE, 1996, pp. 260–265. doi:10.1109/ISIE.1996.548429.
URL http://ieeexplore.ieee.org/document/548429/

[49] L. Olcomendy, A. Pirog, Y. Bornat, J. Cieslak, D. Gucik-Derigny, D. Henry, B. Catargi, S. Renaud, Tuning of an Artificial Pancreas Controller: An in silico methodology based on clinically-relevant criteria, Proceedings of the Annual International Conference of the IEEE Engineering in Medicine and Biology Society, EMBS 2020-July (2020) 2544–2547. doi:10.1109/EMBC44109.2020.9175292.

[50] N. Hansen, The CMA Evolution Strategy: A Tutorial (apr 2016). doi:10.48550/ARXIV.1604.00772.

[51] R. Mullor Casero, F. J. Izquierdo Sebastián, Clúster de Cálculo: Rigel [Computing cluster: Rigel] (2020).
URL https://wiki.upv.es/confluence/pages/viewpage.action?pageId=264044546

[52] S. D. Patek, L. Magni, E. Dassau, C. Hughes-Karvetski, C. Toffanin, G. De Nicolao, S. Del Favero, M. Breton, C. D. Man, E. Renard, H. Zisser, F. J. Doyle, C. Cobelli, B. P. Kovatchev, Modular Closed-Loop Control of Diabetes, IEEE Transactions on Biomedical Engineering 59 (11) (2012) 2986–2999. doi:10.1109/TBME.2012.2192930.

[53] F. Reiterer, G. Freckmann, Advanced carbohydrate counting: An engineering perspective, Annual Reviews in Control 48 (2019) 401–422. doi:10.1016/j.arcontrol.2019.06.003.

[54] T. Lumley, leaps: Regression Subset Selection (based on Fortran code by Alan Miller) (2020).
URL https://cran.r-project.org/package=leaps

[55] R Core Team, R: A Language and Environment for Statistical Computing, R Foundation for Statistical Computing, Vienna, Austria (2021).
URL https://www.r-project.org/

[56] M. Kuhn, caret: Classification and Regression Training (2021).
URL https://cran.r-project.org/package=caret

[57] G. Franklin, J. Powell, M. Workman, Digital Control of Dynamic Systems, Addison-Wesley series in electrical and computer engineering: Control engineering, Addison-Wesley Publishing Company, 1990.
URL https://books.google.es/books?id=lw8oAQAAMAAJ

[58] M. Schiavon, C. D. Man, Y. C. Kudva, A. Basu, C. Cobelli, In Silico Optimization of Basal Insulin Infusion Rate during Exercise: Implication for Artificial Pancreas, Journal of Diabetes Science and Technology 7 (6) (2013) 1461–1469. doi:10.1177/193229681300700606.

[59] T. Battelino, T. Danne, R. M. Bergenstal, S. A. Amiel, R. Beck, T. Biester, E. Bosi, B. A. Buckingham, W. T. Cefalu, K. L. Close, C. Cobelli, E. Dassau, J. H. DeVries, K. C. Donaghue, K. Dovc, F. J. Doyle, S. Garg, G. Grunberger, S. Heller, L. Heinemann, I. B. Hirsch, R. Hovorka, W. Jia, O. Kordonouri, B. Kovatchev, A. Kowalski, L. Laffel, B. Levine, A. Mayorov, C. Mathieu, H. R. Murphy, R. Nimri, K. Nørgaard, C. G. Parkin, E. Renard, D. Rodbard, B. Saboo, D. Schatz,

K. Stoner, T. Urakami, S. A. Weinzimer, M. Phillip, Clinical Targets for Continuous Glucose Monitoring Data Interpretation: Recommendations From the International Consensus on Time in Range, Diabetes Care 42 (8) (2019) 1593–1603. doi:10.2337/dci19-0028.

[60] S. G. Luke, Evaluating significance in linear mixed-effects models in R, Behavior Research Methods 49 (4) (2017) 1494–1502. doi:10.3758/s13428-016-0809-y.

[61] D. J. Barr, R. Levy, C. Scheepers, H. J. Tily, Random effects structure for confirmatory hypothesis testing: Keep it maximal, Journal of Memory and Language 68 (3) (2013) 255–278. doi:10.1016/j.jml.2012.11.001.

[62] D. J. Hand, Understanding The New Statistics: Effect Sizes, Confidence Intervals, and Meta-Analysis by Geoff Cumming, Vol. 80, Taylor & Francis, 2012. doi:10.1111/j.1751-5823.2012.00187_26.x.

[63] J. W. White, A. Rassweiler, J. F. Samhouri, A. C. Stier, C. White, Ecologists should not use statistical significance tests to interpret simulation model results, Oikos 123 (4) (2014) 385–388. doi:10.1111/j.1600-0706.2013.01073.x.

[64] M. Koller, Robustlmm: An R package for Robust estimation of linear Mixed-Effects models, Journal of Statistical Software 75 (1) (2016). doi:10.18637/jss.v075.i06.

[65] S. Ahmad, C. M. Ramkissoon, A. Beneyto, I. Conget, M. Giménez, J. Vehi, Generation of Virtual Patient Populations That Represent Real

Type 1 Diabetes Cohorts, Mathematics 9 (11) (2021) 1200. doi:10.3390/math9111200.

[66] J. J. Ruegemer, R. W. Squires, H. M. Marsh, M. W. Haymond, P. E. Cryer, R. A. Rizza, J. M. Miles, Differences Between Prebreakfast and Late Afternoon Glycemic Responses to Exercise in IDDM Patients, Diabetes Care 13 (2) (1990) 104–110. doi:10.2337/DIACARE.13.2.104.

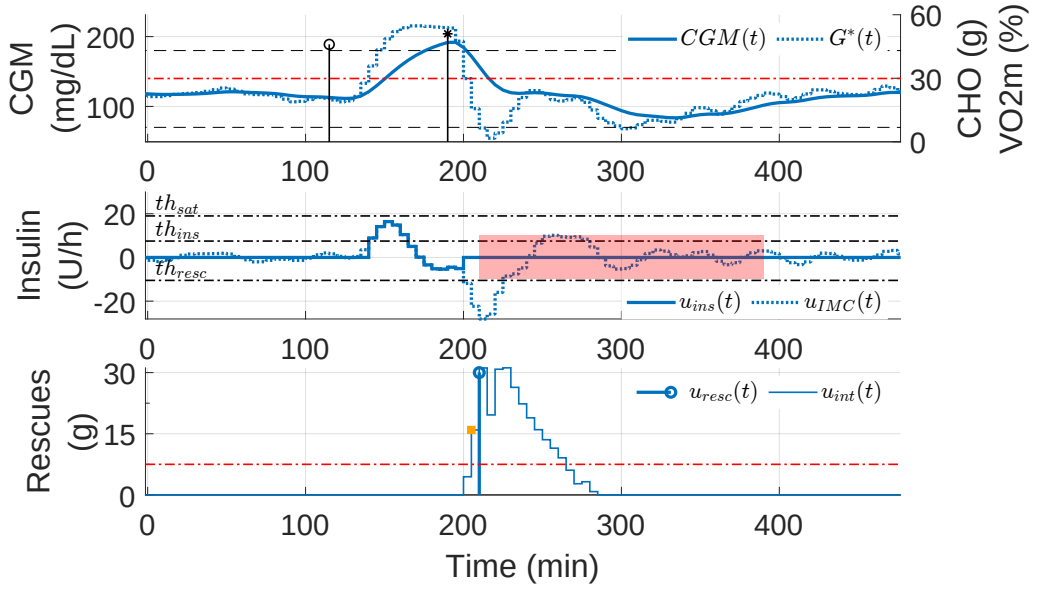


Figure 3: **Control logic to compensate for exercise**. The switching logic converts the negative insulin of the IMC ($u_{IMC}(t)$, middle panel) into a continuous carbohydrate signal ($u_{int}(t)$, bottom panel). If the predicted glucose ($G^*(t)$, upper panel) is in hypoglycemia and $u_{int}(t) \geq 7.5$ (dashed red line in bottom panel), the algorithm suggests a rescue $u_{resc}(t)$ (bottom panel) by quantizing $u_{int}(t)$. Orange squares illustrate that rescue carbohydrates are inhibited if no hypoglycemia risk exists. Insulin $u_{ins}(t)$ is inhibited after the rescue carbohydrate suggestion (red area in the bottom panel). Note that $u_{ins}(t)$ is in deviation form regarding the main controller output signal (i.e., the signal $u_{mc}(t)$ of Figure 1) was allowed to be negative (Phase 3 of Section 2.2.1) to reduce the insulin infusion of the main controller ($u_{mc}(t)$). However, $u_{mc}(t) + u_{ins}(t)$ will be saturated to 0 if $u_{mc}(t) < u_{ins}(t)$.

| | $adjR^2$ | $RMSE_{loocv}$ |
|---|---|---|
| $\hat{k} = 14.2 + 6.17 \cdot 10^{-2} \cdot TDI - 2.59 \cdot u_b -$ $- 1.61 \cdot 10^{-3} \cdot BW \cdot CF + 3.93 \cdot 10^{-3} \cdot BW \cdot CR -$ $- 4.67 \cdot 10^{-3} \cdot CF \cdot TDI - 6.57 \cdot 10^{-3} \cdot CR \cdot TDI$ | 0.972 | 0.0471 |
| $t\hat{h}_{ins} = -51.6 + 28.9 \cdot CR + 0.872 \cdot BW \cdot u_b -$ $- 2.53 \cdot 10^{-2} \cdot BW \cdot CF - 12.9 \cdot CR \cdot u_b -$ $- 0.226 \cdot CF \cdot CR$ | 0.752 | 1.95 |
| $t\hat{h}_{sat} = 4.01 \cdot 10^2 - 1.05 \cdot 10^2 \cdot u_b - 20.8 \cdot CR -$ $- 8.82 \cdot 10^{-2} \cdot BW \cdot CF + 0.209 \cdot BW \cdot CR +$ $+ 0.150 \cdot CF \cdot CR$ | 0.890 | 3.16 |
| $\hat{k}_{resc} = -3.02 - 7.6 \cdot 10^{-2} \cdot CR + 3.11 \cdot 10^{-4} \cdot BW \cdot TDI -$ $- 1.74 \cdot 10^{-2} \cdot BW \cdot u_b + 1.76 \cdot 10^{-4} \cdot BW \cdot CF +$ $+ 8.18 \cdot 10^{-2} \cdot CF \cdot u_b$ | 0.776 | 0.0676 |
| $t\hat{h}_{resc} = -12.3 - 0.133 \cdot BW - 0.295 \cdot TDI +$ $+ 0.103 \cdot BW \cdot u_b + 1.48 \cdot 10^{-2} \cdot CF \cdot TDI -$ $- 2.55 \cdot 10^{-3} \cdot CF \cdot CR$ | 0.955 | 0.209 |

Table 4: **Regression equations of the controller's parameters and related goodness of fit metrics** Evaluated metrics are the adjusted coefficient of determination ($adjR^2$) for multivariable regression models and root-mean-squared error of the leave-one-out cross-validation ($RMSE_{loocv}$). The five models have a low $RMSE_{loocv}$ and acceptable coefficients of determination.

| | NoComp | Hybrid | MD | mIMC |
|---|---|---|---|---|
| **Overall** | | | | |
| Mean CGM (mg/dL) | 161.6 [158.9, 189.5] | 140.6 [139.0, 154.2] | 141.8 [139.0, 145.6] | 140.0 [132.9, 144.8] |
| CV (%) | 30.5 [28.7, 33.7] | 25.2 [23.4, 26.5] | 25.8 [24.4, 29.2] | 25.2 [24.4, 28.6] |
| *% of time CGM* | | | | |
| $>$ 250 mg/dL (%) | 8.2 [4.8, 19.5] | 1.2 [0.3, 2.3] | 1.9 [0.7, 4.0] | 1.4 [0.3, 2.3] |
| $>$ 180 mg/dL (%) | 31.8 [29.9, 45.2] | 16.0 [13.6, 24.1] | 17.3 [16.2, 20.4] | 14.7 [11.8, 22.1] |
| 70-180 mg/dL (%) | 68.2 [54.8, 70.1] | 84.0 [75.9, 86.4] | 81.9 [79.3, 83.8] | 85.1 [77.9, 88.1] |
| $<$ 70 mg/dL (%) | 0.0 [0.0, 0.0] | 0.0 [0.0, 0.0] | 0.0 [0.0, 0.1] | 0.0 [0.0, 0.1] |
| $<$ 54 mg/dL (%) | 0.0 [0.0, 0.0] | 0.0 [0.0, 0.0] | 0.0 [0.0, 0.0] | 0.0 [0.0, 0.0] |
| Daily insulin (U) | 34.7 [29.8, 37.4] | 38.6 [34.0, 41.3] | 38.3 [32.9, 39.9] | 38.5 [34.1, 41.4] |
| **Postprandial control** | | | | |
| *% of time CGM* | | | | |
| $>$ 250 mg/dL (%) | 17.5 [9.4, 28.3] | 2.6 [0.9, 4.2] | 5.1 [1.7, 9.4] | 3.5 [0.7, 5.9] |
| $>$ 180 mg/dL (%) | 57.2 [49.1, 62.3] | 34.0 [25.7, 35.5] | 41.4 [37.6, 47.5] | 34.9 [29.4, 45.5] |
| $<$ 70 mg/dL (%) | 0.0 [0.0, 0.0] | 0.0 [0.0, 0.0] | 0.0 [0.0, 0.0] | 0.0 [0.0, 0.0] |
| $<$ 54 mg/dL (%) | 0.0 [0.0, 0.0] | 0.0 [0.0, 0.0] | 0.0 [0.0, 0.0] | 0.0 [0.0, 0.0] |
| Meals needing rescues(%) | | – | – | 0.0 [0.0, 1.1] |
| Mean rescues (g) | – | – | – | 15.0 [15.0, 15.0] |

Table 5: **Performance metrics of meal compensation.** Four meal compensation techniques, which share the same main controllers, were compared: absence of meal compensation (NoComp), announced-based compensation (Hybrid), meal-detector-based compensation (MD), and proposed approach (mIMC). Metrics are expressed in median [25th percentile, 75th percentile] of the 10 virtual adults. "Overall" metrics aggregate the entire simulation period (30 days), while "Postprandial control" metrics refer to a specific period of the postprandial: percent of time-related metrics aggregate the 3-h period after the meal, and rescue-related metrics aggregate the meal-to-meal period.

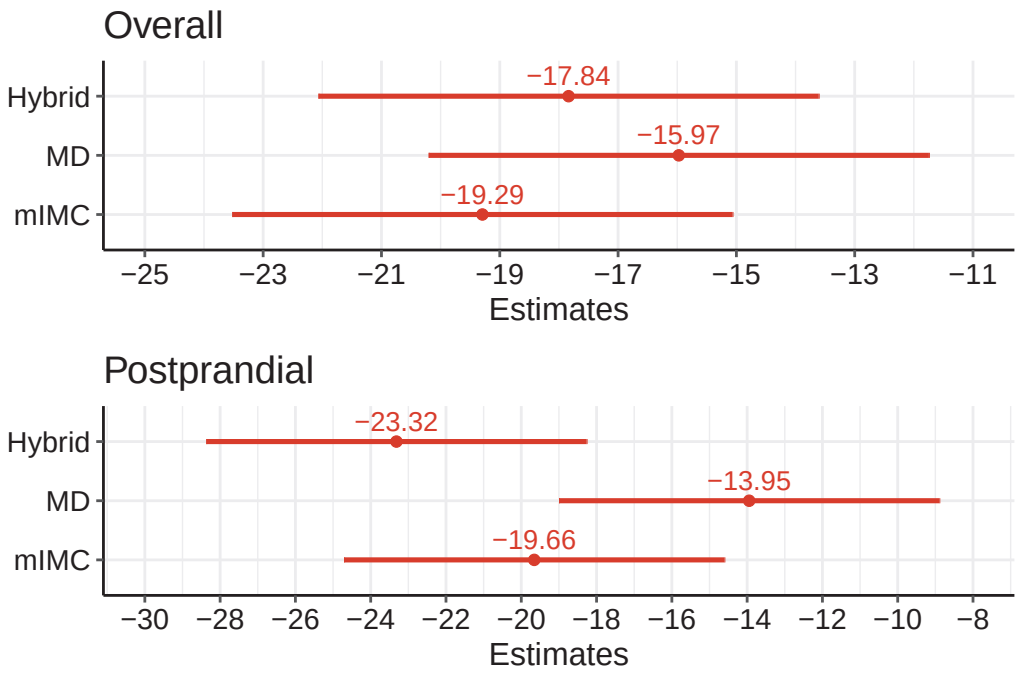


Figure 4: **Mean difference of the percentage time above 180 mg/dL regarding the controller without meal compensation (NoComp)**. Red text labels indicate the mean difference between every controller with meal compensation (Hybrid, MD, mIMC) and NoComp obtained using robust random-intercept models. Lines represent the Wald 95%-interval confidence. The upper panel refers to the percentage time of CGM above 180 mg/dL within the 30 days of simulation, while only the 3 h after each meal are considered in the bottom panel.

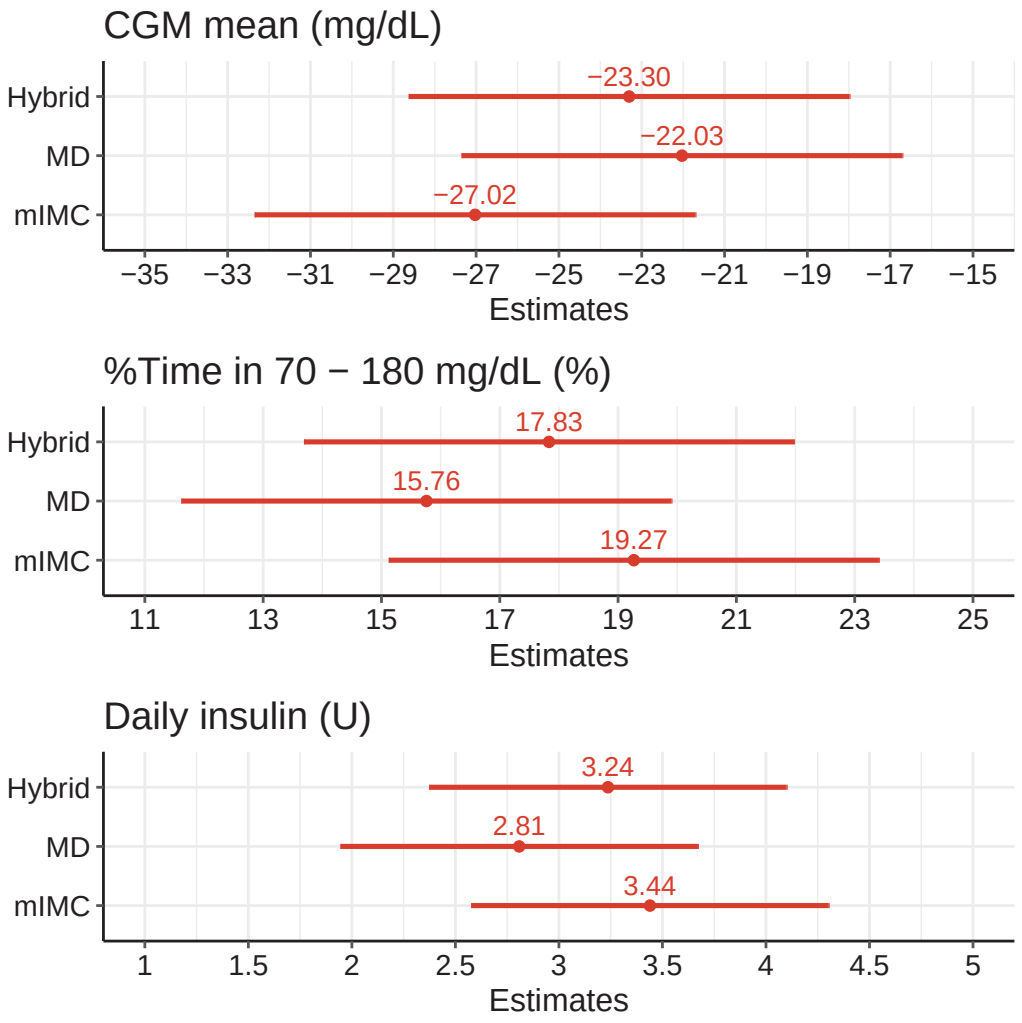


Figure 5: **Mean difference of CGM mean, time in range, and daily insulin regarding the controller without meal compensation (NoComp)**. Red text labels indicate the mean difference between every controller with meal compensation (Hybrid, MD, mIMC) and NoComp obtained using robust random-intercept models. Lines represent the Wald 95%-interval confidence. The upper panel refers to the CGM mean, the middle panel to the percent time in 70 –180 mg/dL, and the bottom panel to the daily insulin. All metrics correspond to the 30 days of the simulation.

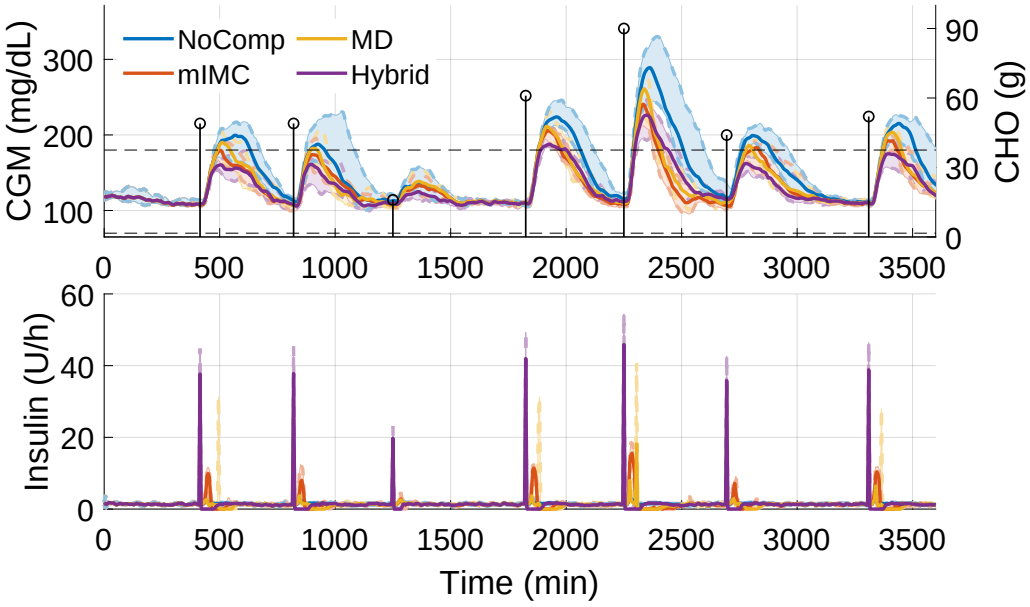


Figure 6: **Populational glucose and insulin profiles of Scenario A**. It shows 2 of the 30 days of the simulation comparing four meal compensation techniques: absence of meal compensation (NoComp), announced-based compensation (Hybrid), meal-detector-based compensation (MD), and proposed approach (mIMC). The solid lines represent the median of the 10 virtual adults, the shaded area is the interquartile range, and the dashed lines are the 25th and 75th percentiles. The black circles in the upper panel represent meal events whose carbohydrate contents are shown on the right axis.

| | NoExComp | MD | mIMC |
|---|---|---|---|
| **Overall** | | | |
| Mean CGM (mg/dL) | 138.2 [132.1, 141.7] | 136.9 [135.6, 138.5] | 141.9 [136.5, 146.2] |
| CV (%) | 33.3 [31.4, 34.4] | 34.1 [33.1, 35.1] | 29.6 [27.4, 32.0] |
| *% of time CGM* | | | |
| $>$ 250 mg/dL (%) | 1.6 [0.8, 2.9] | 2.2 [1.5, 3.6] | 1.6 [1.0, 2.9] |
| $>$ 180 mg/dL (%) | 19.2 [13.5, 21.1] | 19.2 [18.1, 20.6] | 19.8 [13.6, 20.8] |
| 70 – 180 mg/dL (%) | 75.5 [72.7, 81.5] | 76.5 [71.6, 77.0] | 79.6 [77.5, 85.5] |
| $<$ 70 mg/dL (%) | 5.3 [4.5, 6.6] | 4.6 [4.0, 5.1] | 0.9 [0.4, 1.1] |
| $<$ 54 mg/dL (%) | 3.7 [2.2, 4.1] | 2.8 [2.0, 3.4] | 0.0 [0.0, 0.0] |
| Daily insulin (U) | 37.9 [33.0, 40.7] | 37.6 [31.8, 39.6] | 37.7 [33.2, 40.6] |
| Daily CHO (g) | 0.0 [0.0, 0.0] | 0.0 [0.0, 0.0] | 27.5 [23.9, 31.0] |
| **Exercise control** | | | |
| *% of time CGM* | | | |
| $>$ 140 mg/dL (%) (resc) | – | – | 9.6 [5.6, 12.8] |
| $<$ 70 mg/dL (%) | 38.3 [34.6, 44.1] | 34.7 [30.7, 39.2] | 6.5 [3.0, 8.7] |
| $<$ 54 mg/dL (%) | 27.0 [17.0, 30.4] | 21.6 [16.1, 26.4] | 0.1 [0.0, 0.3] |
| Events with rescues (%) | – | – | 96.7 [96.7, 96.7] |
| Mean rescues (g) | – | – | 27.2 [23.7, 31.0] |

Table 6: **Performance against exercise.** It includes the results of three controllers: the meal-detector-based controller (MD), the proposed controller (mIMC), and the proposed controller disabling the rescue suggestion module (NoExComp). Metrics are expressed in median [25th percentile, 75th percentile] of the 10 virtual adults. "Overall" metrics aggregate the entire simulation period (30 days), while "Exercise control" metrics refer to a specific period after the exercise: percent of time-related metrics aggregate the 3-h period after the exercise, and rescue-related metrics aggregate the exercise-to-exercise period.

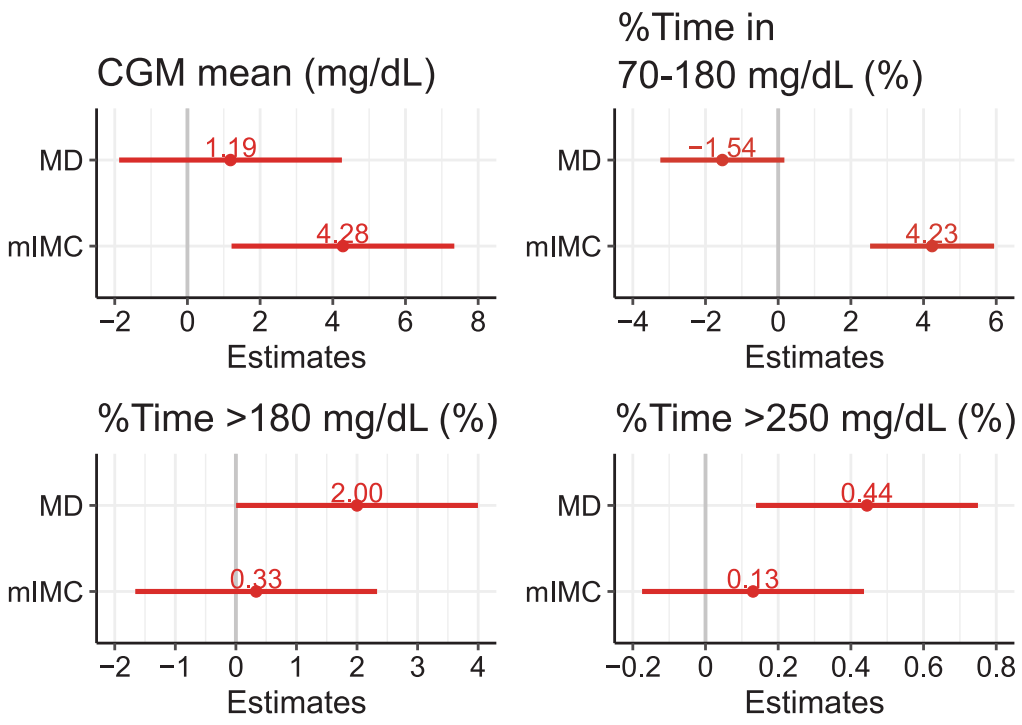


Figure 7: **Mean difference of CGM mean, time in range, and time in hyperglycemia regarding the controller without exercise compensation (NoExComp)**. Red text labels indicate the estimated mean difference of the controllers MD and mIMC regarding the controller NoExComp obtained using robust random-intercept models. Lines represent the Wald 95%-interval confidence. All metrics correspond to the 30 days of the simulation.

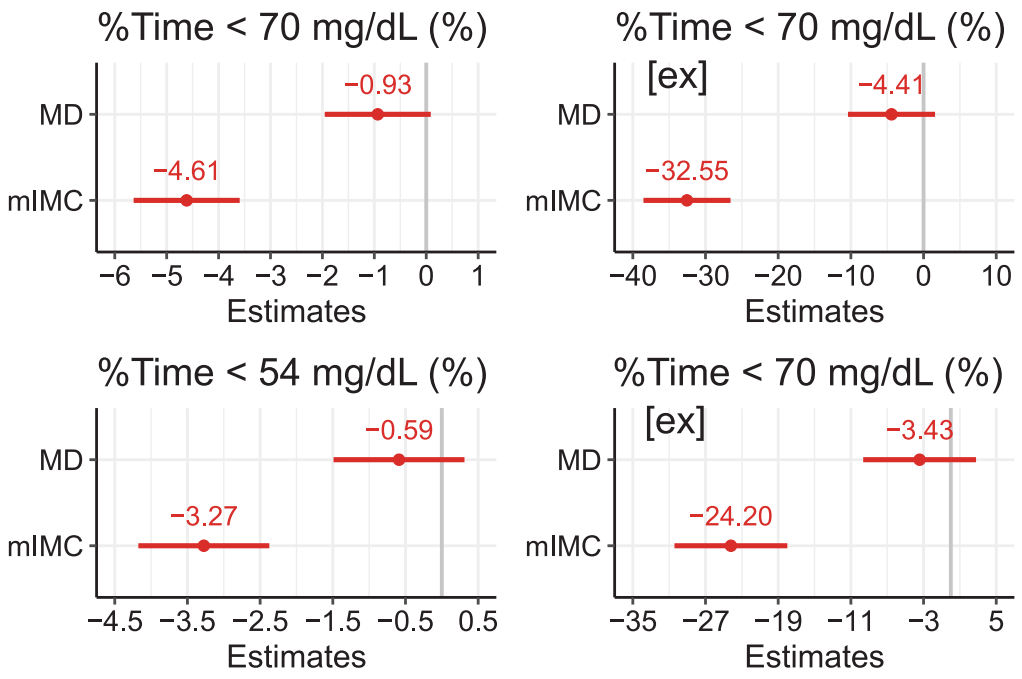


Figure 8: **Mean difference of time in hypoglycemia regarding the controller without exercise compensation (NoExComp)**. Red text labels indicate the estimated mean difference between the controllers MD and mIMC, and the controller NoComp using robust random-intercept models. Lines represent the Wald 95%-interval confidence. The term "ex" added to the name of the metrics denotes that the metric corresponded to the first 3 h after each exercise event, while the remaining metrics considered the 30 days of the simulation.